

# NUMERICAL FLEET OPTIMIZATION STUDIES FOR IMPROVED COMPATIBILITY

**Paul Lemmen**

**Cor van der Zweep**

**Floris Leneman**

TNO Automotive

The Netherlands

**Paul Altamore**

TNO-MADYMO North America

United States

Paper No. 445

## ABSTRACT

On behalf of NHTSA and the Dutch Ministry of Traffic and Transport the Safety department of TNO Automotive is performing numerical fleet studies using multi-body models. Aim is to develop strategies for optimization of front-end structures minimizing the total harm in car-to-car crashes on a fleet-wide basis. For these studies multi-body models are being constructed from existing finite element models. Front-end structure and passenger cell are modeled in detail to provide realistic deformation modes. Furthermore dummies, airbags, belts and main interior parts like dashboard and steering wheel are included. Currently four models are available, each of a different vehicle class.

To indicate the performance of the multi-body vehicle models for crashworthiness optimization of a fleet a study on offset frontal impacts is performed. Using the multi-body models a series of parameter sweeps over relevant accident and design parameters were performed. The accident parameters included vehicle type, belt usage and occupant size. The design parameters relate to the front-end geometry of the two smaller vehicles and the front-end stiffness of all vehicles. A total set of 2500 scenarios was simulated.

## INTRODUCTION

Compatibility is an important subject in road traffic safety research, because in many accidents more than one road user is involved. In that case the passive safety of the different road users is often in unbalance. This leads to an incompatible situation in which one of the parties suffers from the relative aggressiveness of the other. A solution to this problem may be found in improved vehicle compatibility which combines self and partner protection characteristics. During the last decades extensive research was done on the statistics of car-to-car crashes giving a/o interesting rates of aggressiveness [1,2]. Although the occupant safety has improved significantly car-to-car crashes form an increasingly important class of accidents to be examined making it one of the most important safety issues for the car industry and governmental bodies [1,3, 4, 5, 9].

There are two main injury-causing aspects to car collisions in general but also with respect to compatibility:

excessive deceleration and intrusions [8]. The deceleration aspects relate to the phenomenon that lighter cars undergo larger decelerations than heavier cars in a collision between both. So, in the lighter car the occupants can get injured more easily, due to these large decelerations and contacts directly resulting from these decelerations. On the other hand, intrusions relate to entering of structural car parts into the passenger cabin that should be avoided as much as possible. A first important step to avoid intrusions is the avoidance of geometrical mismatch. Shearlaw and Thomas [6] show that it is very difficult to tackle the question whether or not cars are compatible with respect to these intrusion effects.

Furthermore, the passenger compartment integrity should be preserved as much as possible: collapse of the compartment should be avoided. For this purpose, the global strength of the passenger compartment should be larger than the strength of the front and of course large enough to withstand the forces during the whole crash. This also means that the strength of two cars in a crash should be optimized such, that the collision energy is dissipated without compartment collapse of any of the cars [3]. Of course, the strengths of the cars are closely related to the deceleration of the cars.

When assessing compatibility the overall safety of a fleet should be considered. For the evaluation of the overall safety of an automotive fleet systems modeling approaches have been developed. In the nineteen-seventies Ford Motor Company developed a method for maximizing a single vehicle's safety performance in frontal crashes [10]. This program was updated by the University of Virginia to include new biomechanical transforms and updated accident data as well as multivariable analysis capability [11]. Other car manufacturers also developed programs, mainly for optimizing single vehicle design. On behalf of NHTSA Volpe developed a model that predicts the total harm over a range of vehicle types rather than a single subject vehicle [12]. The model estimates injuries over a given set of crashes considering air bags, seat belts and occupants of varying size. It incorporates updated accident data for the statistical accident environment model and injury risk functions that convert injury measures into the AIS scale [14]. Injury values are obtained from MADYMO occupant kinematic models of a car and LTV loaded by crash pulses obtained from one-dimensional lumped parameter models. Figure 1 summarizes the methodology.

The method does not include an optimization strategy to minimize the overall Harm in a fleet environment.

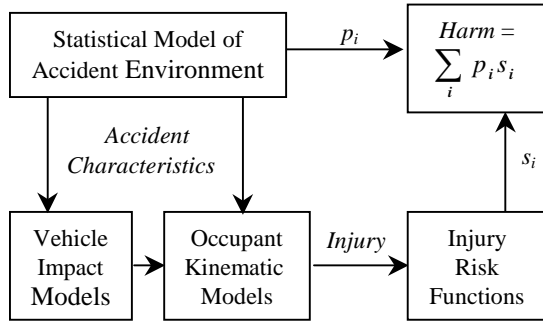


**Figure 1.** Fleet Systems Model Methodology [12]

Ideally injury values are to be computed using detailed vehicle FE models. However, while potentially very accurate these are computationally too expensive to execute for fleet systems models that a substantial amount of simulations [15]. Alternatively simpler but faster running lumped mass models in MADYMO may be used. Although less accurate these models require substantially less computer time making it easier to conduct the necessary simulations. The models were successfully applied in numerical optimization studies bringing all injury levels in a small fleet (limited number of scenarios) below critical values by adjustment of the frontal stiffness [9, 16]. The result was obtained by optimizing the stiffnesses of main load carrying members in the front-ends. Geometrical interaction was not considered, as it could not be translated into a continuous parameter for numerical optimization using direct methods. However, while the front-end stiffness does affect compatibility, geometrical interaction is regarded as the prime factor for good compatibility. Therefore structural variants should be considered in the optimization process which may be stated as [15]

$$\text{Minimize } \text{Inj}(x, u) = p_i s_i(x, u)$$

subject to:

$$\begin{aligned} \text{Wgt}(x) &< \text{Wgtmax} \\ \text{Cost}(x, \text{w}(x)) &< \text{Costmax} \\ x_{\min} &< x < x_{\max} \end{aligned}$$

where:

- $x$  = Vector of design variables
- $u$  = Belt usage rate
- $\text{Inj}(x, u)$  = Total injuries
- $\text{Wgt}(x)$  = Incremental weight for with design 'x'
- $\text{Cost}$  = Incremental cost for  $x$  and  $\text{Wgt}(x)$
- $\text{Wgtmax}$  = Upper constraint on incremental weight
- $\text{Costmax}$  = Upper constraint on incremental costs
- $p_i$  = Probability of event  $i$
- $s_i$  = Injuries resulting from event  $i$

The restraints on the design variables  $x$  are included to limit weight as well as costs of the proposed design modifications and to ensure that modifications remain within realistic ranges. Each crash event  $i$  may be characterized by six accident variables namely vehicle

types, impact mode, impact speed, seat position, occupant size and belt usage [12, 15].

In view of the large number of scenarios to be considered in fleet studies optimization by considering structural variants can only be achieved using design of experiments (DOE) or identical methods that scan the design space by variation of relevant design parameters. Correct interpretation of results requires an adequate formulation of the object or target function.

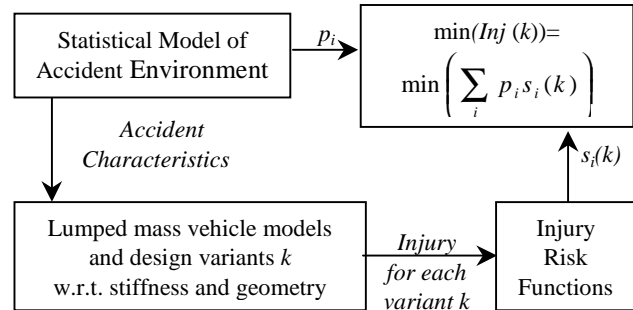


**Figure 2.** Fleet Systems Model Methodology using multi-body vehicle models with occupants

Figure 2 depicts the fleet systems model using multi-body vehicle models to predict injuries. In this paper the vehicle models, the injury risk functions that form the basis of the object function and results of a fleet study considering design variants will be discussed.

## VEHICLE MODEL DEVELOPMENT AND VALIDATION

Based on existing FE models four lumped mass models representative for the US fleet were developed. The vehicles are listed in table 1.

**Table 1.** Available vehicle models

Model	Class	Mass [kg]	Test Mass [kg]
Geo Metro	Subcompact	800	1191
Chrysler Neon	Compact pass.	1085	1371
Ford Taurus	Midsized pass.	1488	1728
Ford Explorer	SUV	1971	2205

The front-ends and the side structures were modeled in detail to describe the actual interaction for frontal and side impacts. The rigid bodies are connected by non-linear spring and damper elements, which represent the stiffness behavior. Characteristics of these elements were derived using FE models and component test data. Attention was focussed on the main load carrying components like longitudinals and shotguns. The occupant compartment intrusion is described using contact surfaces. The interior of the car is modeled including a dashboard, steering wheel, belts, airbag and Hybrid III dummy at the driver side. Figure 3 shows the models of the Ford Taurus and the Chrysler Neon in the undeformed configuration.

Interaction between the vehicles is realized with contact facets at the front and the side.

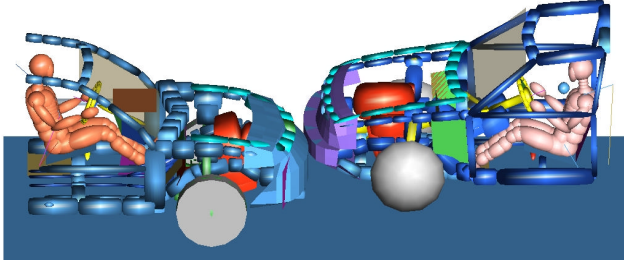


**Figure 3.** Undeformed frame model of Neon Chrysler (left) and Ford Taurus (Right)

The frame models were validated against Full Width barrier NCAP test data. In addition, the vehicle signals are validated against FE simulations under different angles and different crash scenarios. Figure 4 shows typical results for vehicle signals (left) and dummy response (right). Results correlate well.

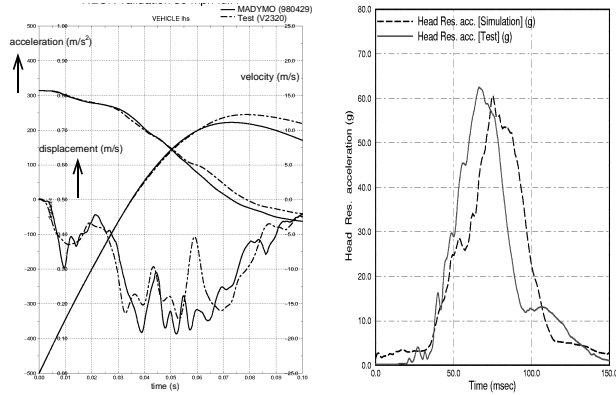


**Figure 4.** Validation frontal Chrysler Neon model: frontal car structure (left) and resultant head acceleration of a 50<sup>th</sup> percentile Hybrid-III (right)

In addition to the vehicle and dummy signals the proposed compatibility measurables were compared. Table 2 compares the Average Height of Barrier Force (AHoBF) which is calculated as follows [17]

$$\begin{aligned}
 AHoF(t) &= \frac{\sum_i (F_i(t) h_i)}{\sum_i F_i(t)} \\
 AHoBF &= \frac{\sum_t \left( AHoF(t) \sum_i F_i(t) \right)}{\sum_t \sum_i F_i(t)}
 \end{aligned} \tag{1}$$

where:

- $F_i$  = Force on cell  $i$
- $h_i$  = height of cell  $i$

Except for the Chrysler Neon all vehicle models show a good correlation with test results. Based on NCAP test data NHTSA has identified AHoBF ranges for different vehicle classes [17]. Results for all vehicle models except the Neon are within the specified class range. Findings for the Neon are currently being investigated in more detail using FE models.

**Table 2.** Comparison of Average Height Of Barrier Force.

Car	AHoBF [m]	AHoBF (NCAP)	Class range [m]
Geo Metro	0.44	0.42 <sup>1)</sup>	0.41 – 0.47
Chrysler Neon	0.51	0.45	0.43 – 0.48
Ford Taurus	0.49	0.50 <sup>1)</sup>	0.43 – 0.50
Ford Explorer	0.58	0.63	0.50 – 0.62

1) Data somewhat different than values indicated by NHTSA in ref. [20]

The Average Height of Barrier Force is known as a relevant measure, however, for compatibility the force distribution on the barrier is even more important. Figure 5 therefore compares load cell data at two time frames for the Ford Taurus.

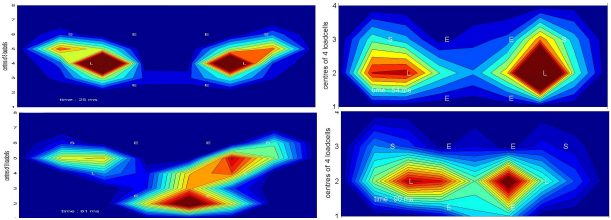


**Figure 5.** Comparison of simulated (left) and experimental (right) load cell wall data for the Ford Taurus at  $t = 25$  ms (top) and  $t = 60$  ms (bottom). Note that the dimensions of the grid sizes in the simulation are somewhat different from the test (simulation: 8\*8; test: 4\*9).

At 25 ms high loads are located at longitudinal locations. Note that the dimensions of the cells and therefore the grid sizes are somewhat different, which may affect the results to some extent. At 60 ms the sub-frame and engine of the simulation model partake in the load transfer which is not the case in the actual test. Despite this discrepancy the simulated results generally correlate very well with experimental data and the models may be regarded adequate for usage in fleet studies.

## INJURY RISK FUNCTIONS

For frontal impacts the most commonly used injury measures include Head Injury Criterion (HIC), Viscous Criterion (VC), 3 millisecond acceleration (3 MS), Combined Thoracic Index (CTI), Femur Force Compression (FFC),  $N_{ij}$ , FNIC, Tibia Index (TI) and TCFC. See also figure 6. All of these injury measures used as regulatory criteria except for the CTI. CTI though is recommended by NHTSA for research use [13].

Prediction of the lower leg injuries requires accurate representation of intrusions, which can only be achieved by use of detailed finite element models with correct geometry and material modeling. The multi-body models have insufficient detail to represent intrusions correctly and therefore TTI and TCFC are not considered here.

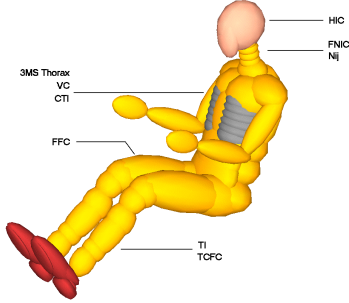


**Figure 6.** Hybrid III 50<sup>th</sup> percentile frontal impact dummy with injury criteria. Except for the lower leg injuries all indicated mechanisms are considered in this study.

Each MADYMO simulation results in a set of injury values for the drivers in both vehicles. To compare risks in the different scenarios results need to be converted into a measure that gives an indication for the overall injury risk (AIR). In previous studies into the optimization of the front-end stiffness this was achieved by summing squared normalized injury values for head, upper leg and chest [16]

$$obj = \sum_i \left( \left( \frac{HIC(i)}{HIC_{crit}(i)} \right)^2 + \left( \frac{FFC(i)}{FFC_{crit}(i)} \right)^2 + \left( \frac{3MS(i)}{3MS_{crit}(i)} \right)^2 \right) \quad (2)$$

The injury values used in eq. (2) were selected based on results of parametric studies [16]. This function was found to be quite effective as it is very discriminative for critical or near critical injuries. Main disadvantage though is that all injuries have identical weights, which is not realistic when considering the harm. Therefore injury significance ratings should be introduced:

$$obj = \sum_i \left( \alpha \left( \frac{HIC(i)}{HIC_{crit}(i)} \right)^2 + \beta \left( \frac{FFC(i)}{FFC_{crit}(i)} \right)^2 + \gamma \left( \frac{3MS(i)}{3MS_{crit}(i)} \right)^2 \right) \quad (3)$$

where  $\alpha$ ,  $\beta$  and  $\gamma$  are the weight factors for the respective injury types. Estimates for the weight factors are provided in table 3. These numbers, based on field studies, were derived in the early nineties to evaluate the performance of restraint systems [18].

**Table 3.** Injury significance factors [18]

Body region	Significance	Weights
Head	60%	$\alpha = 0,60$
Chest	35%	$\beta = 0,35$
Extremities	5%	$\gamma = 0,05$

Alternatively an approach based on the Abbreviated Injury Scale (AIS) may be used, see e.g. [19]. Injury risk functions are used to convert injury values into AIS levels, which subsequently may be transformed into an overall injury risk using the Injury Severity Scale (ISS).

Figure 7 and figure 8 show mathematical models to transfer CTI and HIC values into the AIS probabilities. Identical models have been derived for 3ms, CD, FFC, and Nij. The models, generally known as the injury risk functions, have been proposed by NHTSA on the basis of experimental data and previous research [14]. The experiments were performed within the regulatory range of interest up to critical values. For higher injury values the plotted approximations are therefore more heuristic.

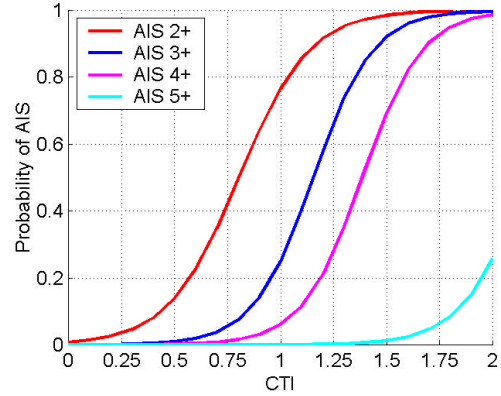


**Figure 7.** Injury risk function for CTI [14]

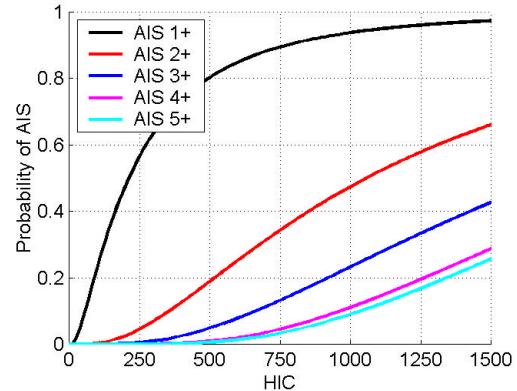


**Figure 8.** Injury risk function for HIC [14]

Mathematical expressions for the injury risk functions can be found on the NHTSA website (<http://www.nhtsa.dot.gov/cars/rules/rulings/AAirBagSNP/RM/PEA/pea-III.n.html>). Using these cumulative functions a vector of AIS probabilities (AIS=0,1,2,3,4,5,6) is obtained by subtracting each AIS probability at the computed injury level from the next AIS probability. For each injury type a vector of AIS probabilities is computed which is converted into an expected AIS value according to

$$E(X) = \sum_{i=1}^6 w_i P_{w_i}(X) \quad (4)$$

where

$X$  = Injury value  
 $E$  = Expected AIS value  
 $P_{w_i}$  = Probability of AIS level  $w_i$   
 $w_i$  = AIS level 0,1,2,3,4,5,6

The expected AIS values for each injury mechanism may be converted into an overall body criterion using normalized cost functions to obtain communal costs (HARM) or using the Injury Severity Scale (ISS) [19]. In this paper the ISS will be used.

## FLEET SETUP AND ACCIDENTS SCENARIOS

To explore the potential of the multi-body models for usage in optimizing the crashworthiness behavior of a fleet a study with four vehicles was performed. Frontal offset impacts at a closure speed of 50 km/h were analyzed in a fleet consisting of the Geo Metro, Neon Chrysler, Ford Taurus and Ford Explorer. Figure 8 shows the accident scenarios. Crashes between the Explorer and the Geo Metro are not considered, as this scenario is strongly incompatible, even when applying the design modifications suggested below. The accident variables occupant size (5<sup>th</sup> percentile female, 50<sup>th</sup> percentile male and 95<sup>th</sup> percentile male) and seat belt usage (belted and unbelted) were varied.

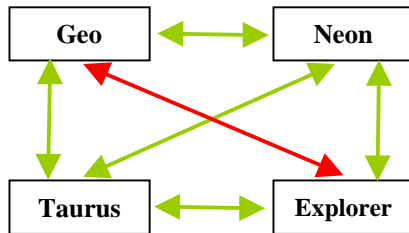


**Figure 8.** Crash scenarios between vehicles. The Explorer Geo scenario is not considered, as it is highly incompatible.

For the optimization two design variables were introduced namely front-end stiffness and front-end geometry. For the stiffness structural components relevant for the crash behavior were identified in each vehicle and related bodies grouped such that their connecting springs and damper characteristics can be changed simultaneously. The scaling of the characteristics corresponds to overall changes in elastic and plastic stiffness of the component. The allowable range of the stiffness was set between 75 and 150% of the original values to be within physically realistic bounds. Weight and cost restraints were not considered here but are largely covered by the above-mentioned restraint. For the front-end geometry design variants of the Geo Metro and the Neon Chrysler were created, see figures 9 and 10. The

depicted modifications are easily implemented in the multi-body models.

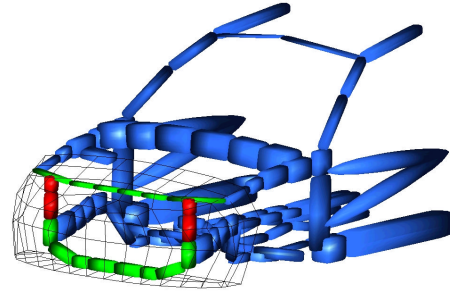


**Figure 9.** Modified front-end Geo Metro. To improve the interaction with other vehicles cross members have been reinforced (Green bodies) and two vertical members linking shotguns and longitudinals (red bodies) have been added.

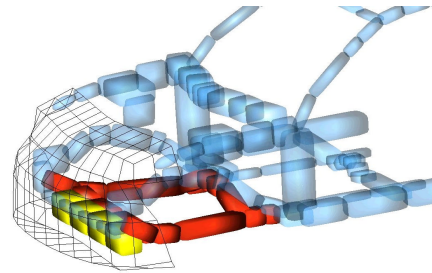


**Figure 10.** Modified front-end Chrysler Neon. To improve the geometrical interaction a sub-frame was added (red bodies) and the lower cross-beam was reinforced (yellow bodies)

## SIMULATION RESULTS

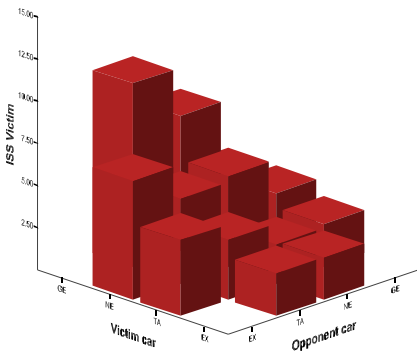
Parametric simulation of all scenarios for relevant design variables yields a total of 2500 individual cases. Here the stiffness for each vehicle is varied in five discrete steps ranging between 75% and 150% of the original stiffness. Each case requires approximately 20 minutes of CPU time on a PC server system. The total required CPU was about 830 hours. For each case a vector of injuries is obtained which is processed into an overall body value using eq. (2) or the alternative method based on AIS and ISS.

Results of the simulations are analyzed with the SPSS statistical program [21]. The computed distributions for the entire subset are shown in figures 10 (ISS) and 11 (weighted squared injuries using eq. (2)). Both figures show identical trends but results based on eq. 2 appear to have larger relative differences which is mainly due to use of squared relative values rather than relative values, see also [16]. This finding may be important for optimization studies as it focuses the search towards critical or near critical cases. However, as it is based on a limited set of accident variants care should be taken when generalizing

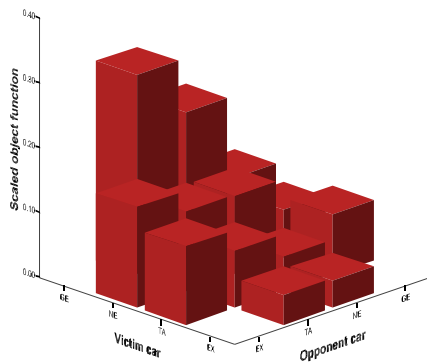
this finding. Therefore ISS will still be used in the sequel of this paper.

To obtain an indication for the contribution of different injuries to these results 3MS, HIC and FFC are plotted in Figure 12 through 14 for the entire subset. FFC values for the smaller vehicles are near or over critical ( $FFC_{crit} = 10000$ ). Chest values are relatively high especially for the smaller cars ( $3MS_{crit} = 60$  g). HIC values are generally low at values up to 400 ( $HIC_{crit} = 1000$ ).

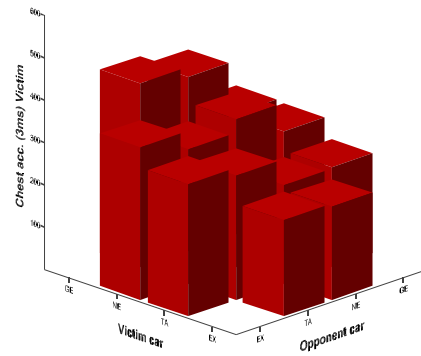
Figure 15 shows ISS values sorted by belt usage. Only limited influence of the belt usage is observed, which is unrealistic. Figure 16 and 17 show FFC and 3MS values. From these figures it is observed that the upper leg load levels for belted drivers are significantly lower as to be as expected. However, 3MS values for the belted drivers are higher than for the unbelted. This is explained by the fact that the belt systems in the vehicle models do not have a load limiter resulting in high chest loads. For a more realistic representation of the fleet behavior a load limiter should be included.



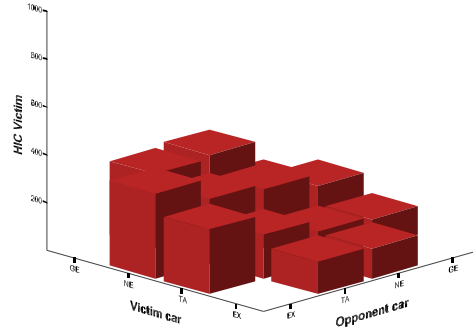
**Figure 11.** ISS distribution (mean values) for entire subset plotted as function of victim and opponent car.



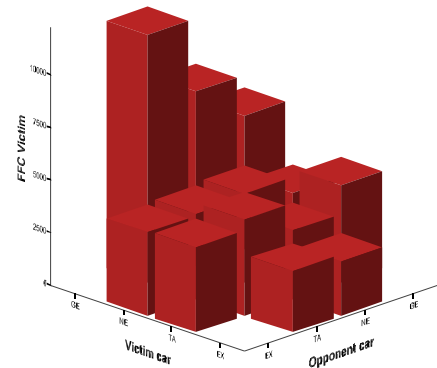
**Figure 12.** Weighted squared injury distribution (mean values) for entire subset plotted as function of victim and opponent car.



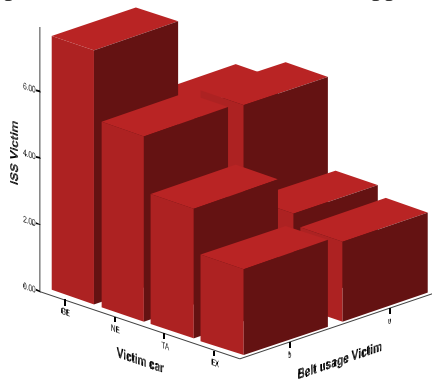
**Figure 13.** 3MS distribution (mean values) of entire subset plotted as function for victim and opponent car.



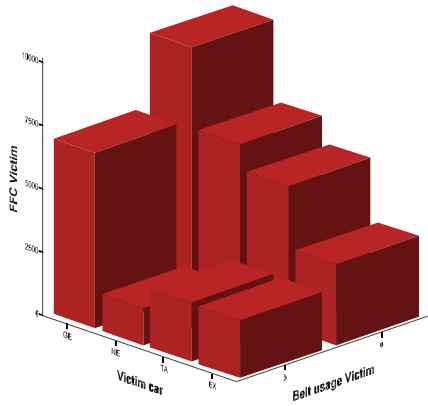
**Figure 13.** HIC distribution (mean values) of entire subset plotted as function of victim and opponent car.



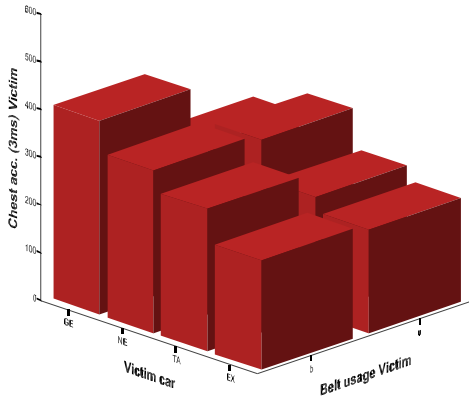
**Figure 14.** FFC distribution (mean values) of entire subset plotted as function of victim and opponent car.



**Figure 15.** ISS distribution (mean values) of entire subset plotted as function of victim car and belt usage.



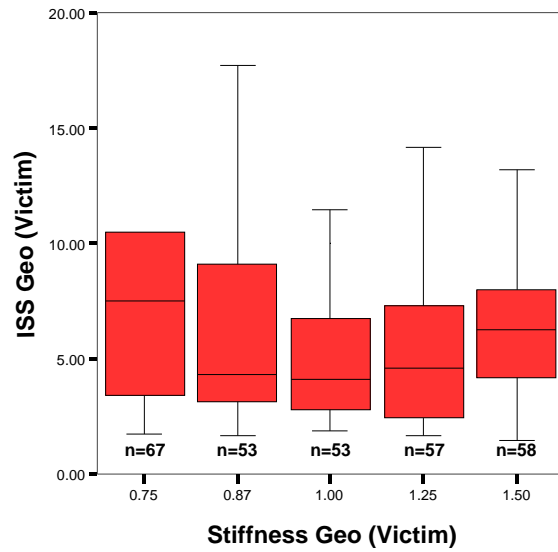
**Figure 16.** FFC distribution (mean values) of entire subset plotted as function of victim car and belt usage.



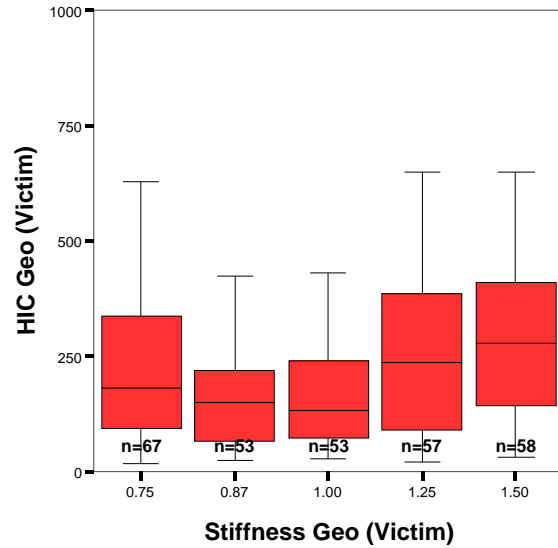
**Figure 17.** 3MS distribution (mean values) of entire subset plotted as function of victim car and belt usage.

Figure 18 shows ISS values of the Geo driver for stiffness variations in the front-end of the Geo. The columns indicate the 25% to 75% range of samples. The vertical lines related to each column indicate ultimate and meridian values. Minimum ISS values occur at the original stiffness. However, when considering separate injuries, figures 19 through 21, different trends are observed. HIC in figure 19 shows an identical behavior as the overall measure. 3MS in figure 20 is fairly insensitive to the front-end stiffness. FFC-left in figure 21 shows a clear reduction with front-end stiffness bringing the 95% range below critical. This trend is not observed in the ISS result due to the relatively low weight factor for FFC. The finding is in agreement with previous studies using direct optimization [9, 16].

Figure 22 and 23 show results of the Geo driver for stiffness variation in the Taurus front-end. The influence on ISS is fairly low but the FFC shows a trend with reduced injury for reduced stiffness of the Taurus front-end, as to be expected.



**Figure 18.** ISS of Geo driver as function of frontal stiffness



**Figure 19.** HIC of Geo driver as function of frontal stiffness

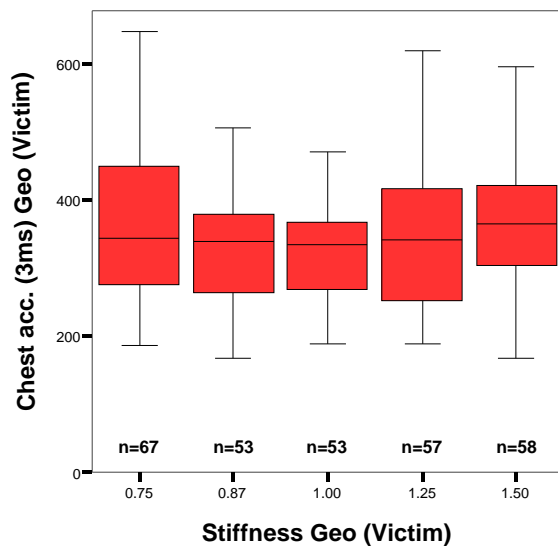


**Figure 20.** 3MS of Geo driver as function of frontal stiffness

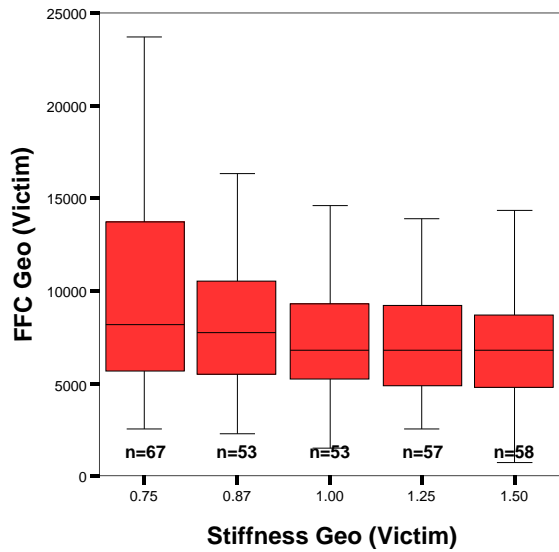


**Figure 21.** 3MS of Geo driver as function of frontal stiffness

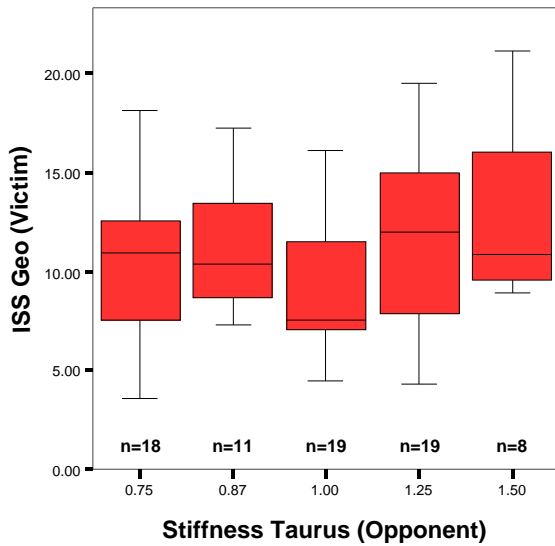


**Figure 22.** ISS of Geo driver as function of frontal stiffness Ford Taurus

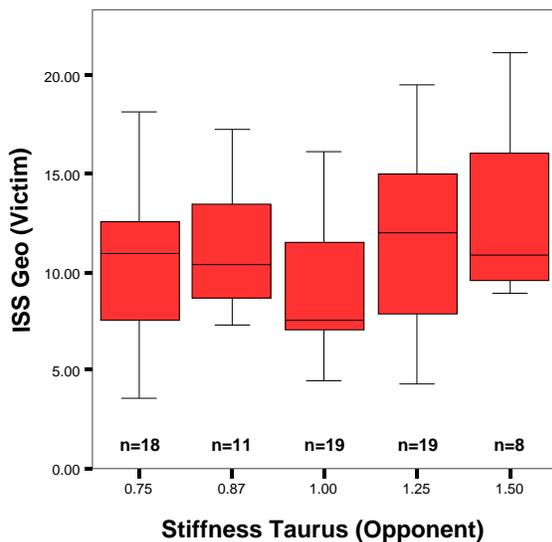


**Figure 23.** FFC of Geo driver as function of frontal stiffness Ford Taurus

Figures 24 through 26 compare injury values between the updated and the original Chrysler Neon. The figures show results for the reference configurations (original stiffness and a belted 50-percentile dummy) only as simulations for the complete statistical study were still in progress at the time of writing. The modification of the front-end depicted in figure 10 was meant to improve the structural interaction and as such reduce intrusions. Knowing the limitations for the lower extremities, results related to upper legs, chest and head are plotted. The results indicate that acceleration related injuries for head and chest remain nearly unaffected whereas intrusion related injuries for the upper legs reduce significantly. The reduction of intrusion becomes clear from figure 27 that shows deformed configurations for the Neon-Geo scenarios. Identical results were found for the adjusted Geo.

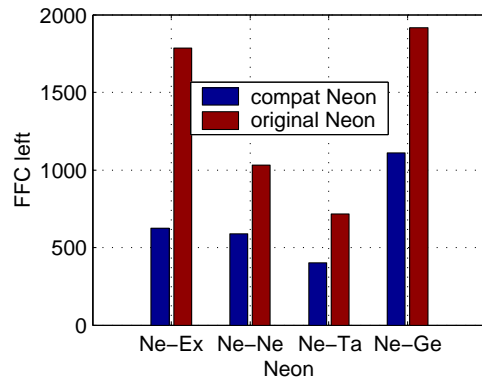


**Figure 24.** FFC values for original and updated Neon for crashes against other cars.

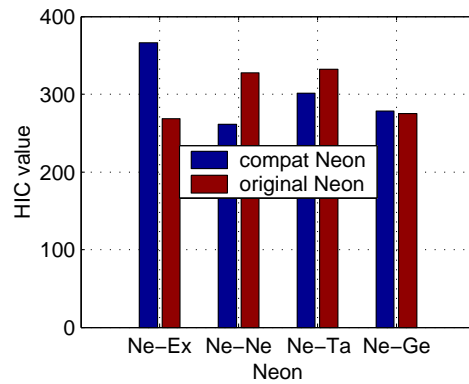


**Figure 25.** HIC values for original and updated Neon for crashes against other cars.

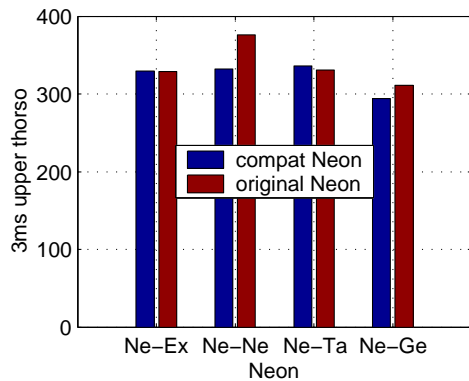


**Figure 26.** 3MS values for original and updated Neon for crashes against other cars.

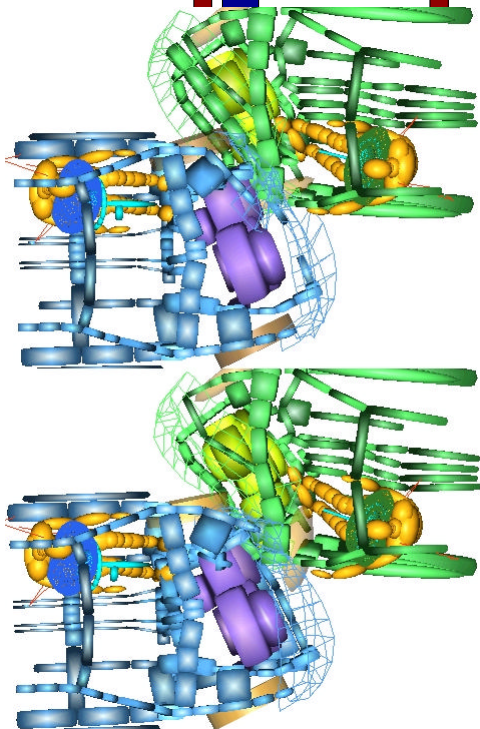


**Figure 27.** Deformed configurations at 80 ms for Neon-Geo scenarios: original Neon (top) and updated Neon (bottom). Neon is blue, Geo is green.

## CONCLUSIONS AND RECOMMENDATIONS

To indicate the performance of the multi-body vehicle models for crashworthiness optimization of a fleet a study on offset frontal impacts was presented. Using models of four different vehicles, that represent the US car fleet, parameter sweeps over relevant accident and design variants were performed.

The vehicle models are 3-D rigid mass models derived from FE models. The rigid bodies are connected by non-linear spring and damper elements representing the stiffness behavior. Main interior parts and dummies are included. Comparison with test results shows that the models provide realistic crash and occupant behavior. The models integrate vehicle and occupant models that were

separated in previous fleet studies. Front-end stiffness and geometry can be adjusted easily by scaling the stiffness of main members and adding new bodies and joints. Although less accurate than finite element models the multi-body models require substantially less CPU making them suitable for the large amount of simulations required in fleet studies.

In the fleet study frontal offset impacts between the four vehicles (Geo Metro, Chrysler Neon, Ford Taurus and Ford Explorer) were considered. Crashes between the different vehicles were simulated with belted an unbelted drivers of different size (5<sup>th</sup> percentile female, 50<sup>th</sup> percentile male and 95<sup>th</sup> percentile male dummies). The front-end stiffness of each vehicle was varied between 75 and 150% of their original value. For the two smallest vehicles design variants that provide improved structural interaction were considered. A full factorial parameter sweep over these accident and design variables resulted in 2500 scenarios where the stiffness of each vehicle was varied in five steps. Simulating these scenarios required an acceptable 830 hours of CPU on a PC server system. Statistical analysis of results showed that injury levels for these considered accident scenario can be reduced below critical values.

Evaluation of results for belt usage showed that the modeling of restraints needs improvements. Despite this the study showed that the models have high potential for this type of fleet studies since they provide realistic vehicle behavior at limited CPU costs. Also structural modifications are easily introduced.

In future work the modeling of the restraint systems should be improved. Comparison of belted and unbelted results showed that the belt models should include load limiters to provide more realistic chest loads. Also the triggering of the airbags should be made dependent on the accident scenario in terms of impact speed and other relevant factors. This allows the simulation of scenarios at different impact speeds. With these improvements fleet studies using scenario weight factors from a statistical accident environment model can be made. Resulting injury distributions can be compared with real world data for validation purposes. In these studies the accident scenarios can be extended, e.g. with side impacts for which validated models are available.

Apart from the fleet modeling work the multi-body models and their improved variants will be employed to improve proposals for compatibility test procedures. Car to barrier simulations with original and improved vehicles will be performed to evaluate proposed barrier design and assessment criteria. This activity will be performed in the European 5<sup>th</sup> framework project VC Compat.

## ACKNOWLEDGEMENTS

The authors wish to thank Jos Huibers from TNO Automotive as well as Gijs Kellendonk and Francois Bronkers from the University of Eindhoven for support in the development of use of the multi-body frame models. They also thank Stephen Summers and Thomas Hollowell of NHTSA as well as Leo Schlosser and Jan Busstra from

the Dutch Ministry of Transport for their support of the compatibility research at TNO.

## REFERENCES

- [1] Hollowell, W.T., and Gabler, H.C., 'NHTSA's Vehicle Aggressivity and Compatibility Research program', 15th Int. Technical Conf. on the Enhanced Safety of Vehicles, Melbourne, Australia, May 13-17, 1996.
- [2] Evans, L., and Frick, M.C., 'Driver fatality risk in two-car crashes -- dependence on masses of driven and striking cars', in Proc. of the 13th ESV Conf., paper no. 91-S1-O-10, Paris, France, 1991.
- [3] Zobel, R., 1997, 'Barrier impact tests and demands for compatibility of passenger vehicles', in: VDI Tagungsbericht 1354, Innovativer Insassenschutz im PKW, pp. 209-225, Düsseldorf, Germany, 1997.
- [4] Faerber, E., 'Improvement of crash compatibility between cars', (project summary), Conference on road infrastructure and safety research in Europe, Risc '97, Brussels, 1997.
- [5] Wykes, N.J., et al., 1998, Accident analyses for the review of the frontal and side impact directives, Report to the European Commission DGIII, TRL, UK.
- [6] Shearlaw, A., and Thomas, P., 'Vehicle to vehicle compatibility in real world accidents', Proc. of the 15th ESV conference, paper no. 96-S4-O-04, 1996.
- [7] H. G. Mooi, J. H. A. M. Huibers (1998). Simple and effective lumped mass model for determining kinetics and dynamics of car-to-car crashes. in: Proc. of Int. Crashworthiness Conf. IJCrash '98, 9-11 September 1998, Delft, The Netherlands.
- [8] H. G. Mooi, T. Nastic., J. H. A. M. Huibers (1999). Modelling and Optimization of Car-to-Car compatibility. VDI berichte NR 1471 (ISBN 3-18-091471-8), pages 239-255, delft, The Netherlands.
- [9] A.W.J. Gielen, H.G. Mooi, J.H.A.M. Huibers (2000). 'An optimization methodology for improving car-to-car compatibility', ImechE transactions C567/047/2000, Delft, The Netherlands
- [10] Ford Motor Co. (1978). 'Safety Systems Optimization Model, Final Report', DOT Report Number DOT HS 6-01446, USA
- [11] K.P. White, H.C. Gabler, W.D. Pilkey and W.T. Hollowell (1985). 'Simulation Optimization of the Crash Worthiness of a Passenger Vehicle in Frontal Collisions using Response Surface Methodology', SAE Paper 850512.
- [12] A.C. Kuchar, R. Greif, G.W. Neat (2001). 'A Systems Methodology For Evaluation of Vehicle Aggressivity In The Automotive Accident Environment', SAE Paper 2001-01-1172
- [13] M. Kleinberger, E. Sun, R. Eppinger, et al. (1998). 'Development of Improved Injury Criteria for the Assessment of Advanced Automotive Restraint system', NHTSA Docket No. 1998-4405-9
- [14] R. Eppinger, E. Sun, et al. (1985). 'Development of Improved Injury Criteria for the Assessment of Advanced Automotive Restraint Systems – II', Supplement to NHTSA Docket No. 1998-4405-9
- [15] S.M. Summers, W.T. Hollowell (2001). 'NHTSA's Crashworthiness Modeling Activities', ESV Paper No. 251
- [16] C.D. van der Zweep, P.L. Lemmen (2002). 'Improvement of Crash Compatibility between Passenger Cars by Numerical Optimisation of Front-end Stiffness', JSAE Paper No. 2002-5353
- [17] S.M. Summers, A. Prasad, W.T. Hollowell (2001). 'NHTSA's Compatibility Research Program Update', SAE Paper No. 2001-01-1167
- [18] D.C. Viano, S. Arepally (1990). 'Assessing the Safety Performance of Occupant Restraint Systems', SAE Paper No. 902328
- [19] J.S.H.M. Wismans, et al. (1994), 'Injury Biomechanics', Course Notes Eindhoven University of Technology No. PRO 1411 – TUE
- [20] <http://www-nrd.nhtsa.dot.gov/> NHTSA's web-page
- [21] SPSS Base 10.0 Applications Guide, SPSS Inc., Chicago, IL, USA, 1999